Quarterly Progress Report

High Temperature Electrochemical Polishing of H2S

from Coal Gasification Process Streams

Grant DE-FG22-94-PC94207

April 1, 1995 - June 30, 1995

by

Professor Jack Winnick

Georgia Institute of Technology

School of Chemical Engineering

Atlanta, GA 30332-0100

MASTER

DISTRIBUTION OF THIS DOCUMENT IS UNLIMITED

DISCLAIMER

Project Objectives

Coal may be used to generate electrical energy by any of several processes, most of which involve combustion or gasification. Combustion in a coal-fired boiler and power generation using a steam-cycle is the conventional conversion method; however total energy conversion efficiencies for this type of process are only slightly over 30%[1]. Integration of a gas-cycle in the process (combined cycle) may increase the total conversion efficiency to 40%[1]. Conversion processes based on gasification offer efficiencies above 50%[1].

H_2S is the predominant gaseous contaminant in raw coal gas. Coal depending on the type and area of extraction can contain up to 5 wt% sulfur, which is converted to gaseous H_2S during gasification. Problems arise due to the corrosive nature of H_2S on metal components contained in these cycles. Because of this, H_2S concentrations must be reduced to low levels corresponding to certain power applications. For example, an integrated coal gasification-combined cycle (IGCC) process producing electricity from coal at nearly 50% overall efficiency[1] incorporates gas turbines that cannot tolerate H_2S levels above 100 ppm. Coal gasification/Molten Carbonate Fuel-Cell(MCFC) systems, achieving conversion efficiencies around 60%[2], function properly only if H_2S is below 1 ppm.

An advanced process for the separation of hydrogen sulfide (H_2S) from coal gasification product streams through an electrochemical membrane is being developed using funds from this grant. H_2S is removed from the syn-gas stream, split into hydrogen, which enriches the exiting syn-gas, and sulfur, which is condensed from an inert sweep gas stream, Figure 1. The process allows removal of H_2S without cooling the gas stream and with negligible pressure loss through the separator. The process is made economically attractive by the lack of need for a Claus process for sulfur recovery. To this extent the project presents a novel concept for improving utilization of coal for more efficient power generation.

Past experiments using this concept dealt with identifying removal of 1-2% H_2S from gases containing only H_2S in N_2[3], simulated natural gas[4,5], and simulated coal gas[6]. Data

obtained from these experiments resulted in extended studies into electrode kinetics and electrode stability in molten melts[7,8,9]. The most recent experiments evaluated the polishing application (removal of H_2S below 10 ppm) using the Electrochemical Membrane Separator (EMS). H_2S removal efficiencies over 90% were achieved at these stringent conditions of low H_2S concentrations proving the technologies polishing capabilities.

Other goals include optimization of cell materials capable of improving cell performance. Once cell materials are defined, cell experiments determining maximum removal capabilities and current efficiencies will be conducted.

Also, a model theoretically describing the preferred reduction of H_2S, the transport of S^{2-}, and the competing transport of CO_2 will be investigated. The model should identify the maximum current efficiency for H_2S removal, depending on variables such as flow rate, temperature, current application, and the total cell potential.

Introduction

The Electrochemical Membrane Separator (E.M.S.), the focus of experimental work, purges a fuel gas contaminated with H_2S. This is done by reducing the most electro-active species in the gas stream. In this case, H_2S is reduced by the following:

$$H_2S + 2e^- \rightarrow H_2 + S^{2-} \qquad (1)$$

A membrane which contains sulfide ions in a molten salt electrolyte will act to transport the ions across to the anode. If the membrane is impermeable to H_2 diffusion from the cathode side, an inert sweep gas can be used to carry the vaporous oxidized sulfur downstream to be condensed.

$$S^{2-} \rightarrow 1/2\ S_2 + 2e^- \qquad (2)$$

Processes to remove H_2S typically rely on low-to -ambient temperature adsorption, followed by sorbent regeneration and Claus plant treatment for conversion of H_2S to a salable by-product, sulfur. Although effective, this type of removal is very process-intensive as well as energy-inefficient due to low temperature operation. Gasification streams generally range from 500°C - 1000°C, requiring cooling before and reheating after process gas sweetening. Although these technologies have proven capable of meeting H_2S levels required by MCFC, there are several disadvantages inherent to these processes[10,11].

Alternative high temperature methods are presently available, but process drawbacks including morphological changes in catalytic beds[12] or inefficient molten salt sorbent processes[13] negate savings incurred through energy efficient removal temperatures.

An electrochemical membrane separation system for removing H_2S from coal gasification product streams is the subject of this investigation. The high operating temperature, flow-through design, and capability of selective H_2S removal and direct production of elemental

4

sulfur offered by this process provide several advantages over existing and developmental H_2S
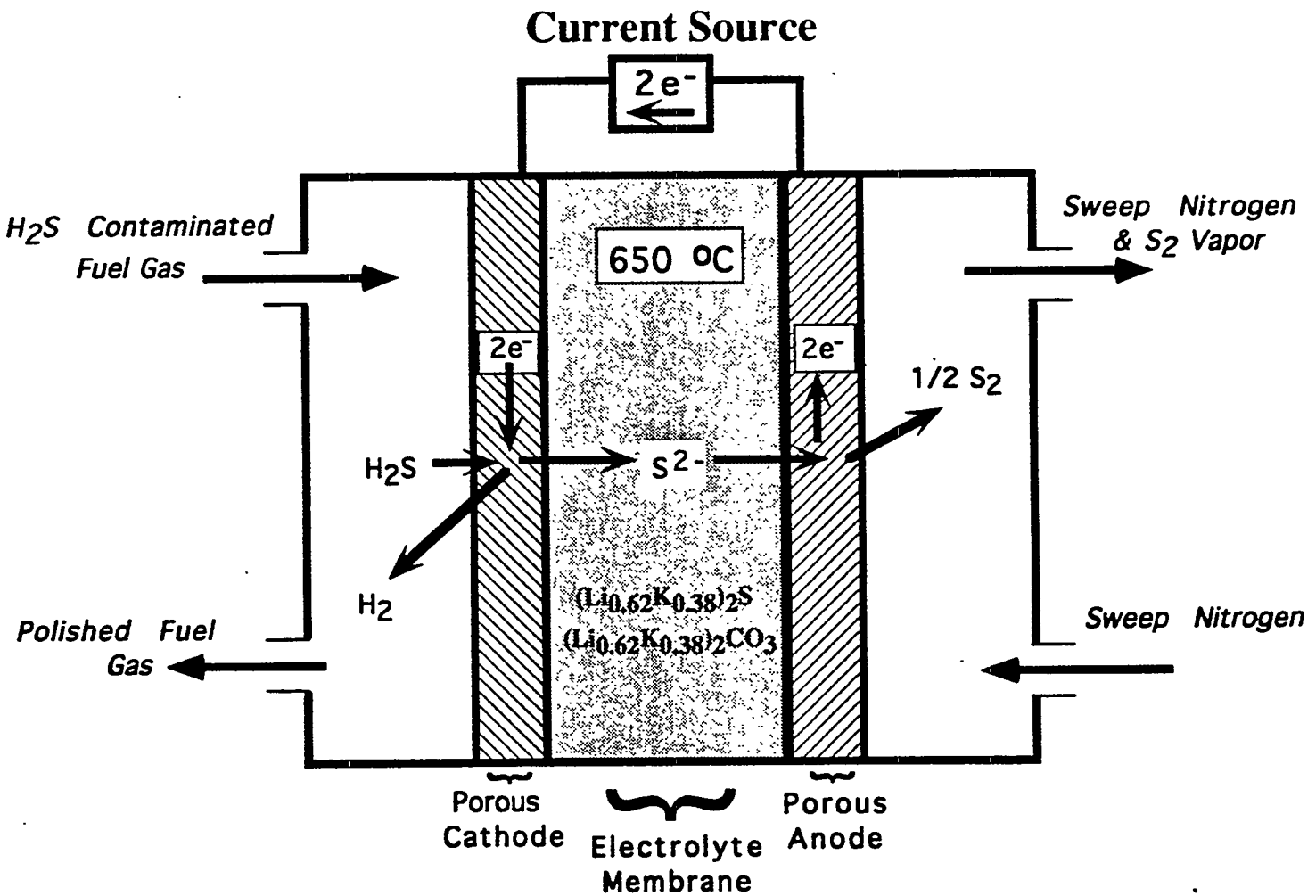
removal technologies.

Current Source

Figure 1. Single-Cell View of the Electrochemical Membrane Separator
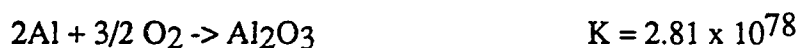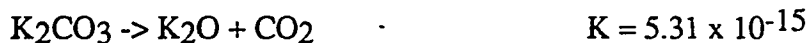
5

Quarterly Research

Electrolyte Management

Electrolyte losses associated with molten carbonate salts is a persistent problem. The mechanism of such losses is not fully understood; CO_2 evolution and reactions with cell materials are possible mechanisms.

Proposed mechanisms for the loss of electrolyte in the E.M.S. are:

1) Material reactions upon process-gas seal formation:

$$2Al + 3/2\ O_2 \rightarrow Al_2O_3 \qquad\qquad K = 2.81 \times 10^{78}$$

$$Al_2O_3 + Li_2CO_3 \rightarrow 2LiAlO_2 + CO_2 \qquad K = 154$$

2) Evaporation at the anode due to a deficiency of CO_2:

$$Li_2CO_3 \rightarrow Li_2O + CO_2 \qquad\qquad K = 2.51 \times 10^{-5}$$

$$K_2CO_3 \rightarrow K_2O + CO_2 \qquad\qquad K = 5.31 \times 10^{-15}$$

3) Evaporation into the surroundings:

$$2Li_2CO_3 + O_2 \rightarrow 2Li_2O_2 + 2CO_2 \qquad K = 3.88 \times 10^{-15}$$

$$2K_2CO_3 + O_2 \rightarrow 2K_2O_2 + 2CO_2 \qquad K = 7.37 \times 10^{-23}$$

with lithium carbonate, comprising 62 mole% electrolyte, being the least stable (larger K).

Quantitative evaporation studies were performed duplicating full-cell conditions[14]. Mechanism (2) & (3) were investigated with evaporation by mechanism (3) entailing the predominant amount of electrolytic losses; 24 hours of exposure evolved on average 30 grams of electrolyte leaving a crystalline residue of Li_2O_2 & Li_2O by:

$$Li_2O_2 \rightarrow Li_2O + 1/2\ O_2 \qquad \Delta G = -41.54\ KJ/mol \quad K = 225$$

Cathode Materials

From results obtained in previous studies, the path to a commercial process is now clear. The primary unresolved components are the cathode and membrane. The cathode must be chemically and mechanically stable in the sulfide/carbonate/hydrogen sulfide environment, and

be electronically conductive at 650°C. Lithium-doped NiO has already proven effective in polishing applications; however, the Ni phase transition to liquid $Ni_{3+x}S_2$ when contacting gas with >100 ppm H_2S, requires alternate cathode materials. Co, which converts to Co_8S_9 in-situ, has recently been shown[15], using Scanning Electron Microscopy(S.E.M.), to be morphologically stable in full cell testing with 100 ppm H_2S. The microscopic view revealed adequate porosity and pore size were maintained in the harsh cell environment. Production of cobalt electrodes in the laboratory is ongoing; consistently manufacturing these electrodes with a pore size and arrangement comparable to the Ni electrodes has been accomplished although current attempts have been less successful. Dry pressing the cobalt powder (d_p = 2 microns) with ~ 40 wt% binder (methylethlycellulose) stabilized the metal in disk form to accomplish the burnout and sintering steps. Stress fractures often occur due to the non-uniform release of binder and apparent temperature inequality within the furnace. These concerns involve the physical aspects of dry pressed powders. Non-uniform distribution of binder material incorporated within the cobalt particles creates particle segregation in certain regions; local density gradients due to disproportionate binder distribution effects the final electrode morphology (i.e. pore size, pore distribution, tortuosity, and crystallographic stability). Adjustments dealing with binder content and temperature cycling will be the impetus of future membrane production as well as improvements in dry-pressing of the cobalt-binder system.

Membrane Materials

Several membranes have been utilized in the EMS since its genesis. MCFC tiles used by Weaver[16], sulfided in-situ, resulted in micro-crack development; however MCFC tile technology will be used in scale-up applications of electrochemical separations, due to success in real-time MCFC. The technology has been refined, but replication in our laboratory is expensive and inefficient for bench-scale testing. Tape-cast membranes of MgO were somewhat more efficient but inconsistent laboratory replication proved detrimental [17]; however, tape casting with zirconia particles still remains a viable option. The most promising membranes for bench-scale

experiments have been manufactured zirconia membranes purchased from Zircar Corporation. Polishing of the gasification streams with these membranes confirms their usefulness; however micro-cracks are still evident from S.E.M. analysis [15], Figure 2, and must be controlled. Alternative laboratory-densified membranes with fiber mats replicating the preprocessed membranes from Zircar Corporation are also being investigated. Positive removal results (over 90% H_2S removal) have been obtained from full-cell testing with these membranes[18]; however, more work is needed to improve the manufacturing techniques. Dry pressing zirconia particles admixed with binder has been the most recent attempt to produce a viable membrane material as well as tape-casting sub-micron ZrO_2 particles in a solvent-binder system.
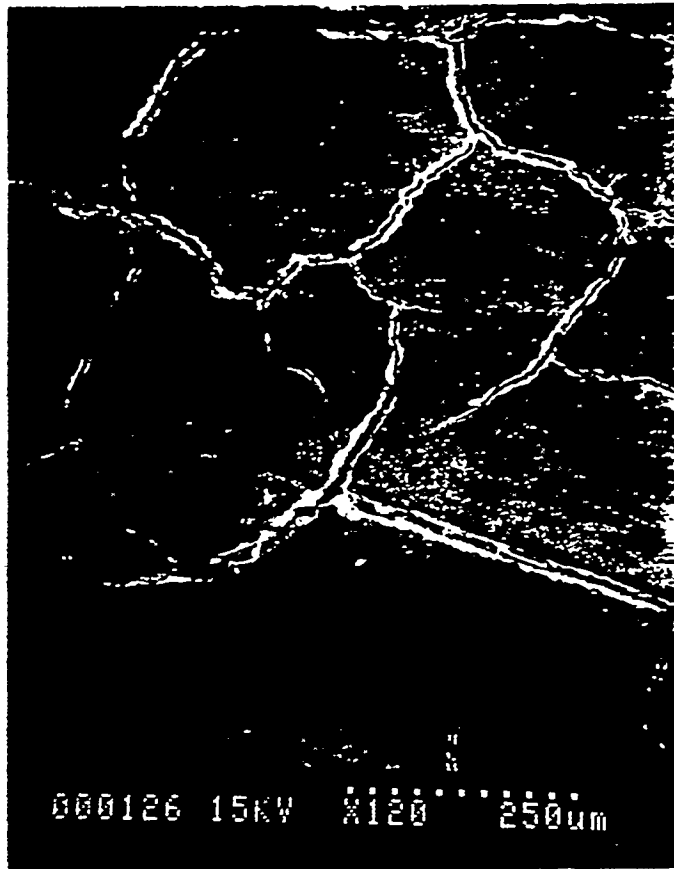

Figure 2. S.E.M. View of a Purchased Zirconia Membrane

Zirconia Cloth-Stabilized Matrices

Continued cell testing will be done utilizing the purchased zirconia membranes along with laboratory-densified zirconia membranes containing zirconia fibers. Laboratory-densified membranes which have proven successful in the past [18] will be tested further. One reason for this is financial. Conventional purchased zirconia membranes cost approximately $ 150.00 per membrane (7.62 cm (3 in) x 7.62 cm (3 in) x 0.063 cm (0.025 in)), compared to $ 10.00 per membrane (7.62 cm (3 in) x 7.62 cm (3 in) x 0.092 cm (0.036 in)) for self-produced membranes.

Laboratory-densified membranes consist of two knit zirconia mats (7.62 cm (3 in) x 7.62 cm (3 in) x 0.0762 cm (0.030 in) purchased from Zircar Corporation. The initial porosity of the mats is approximately 85%. The objective is to fill (rigidize) the knit to a porosity of approximately 65%, which is essential, according to past experiments, in order to operate efficiently[19]. The material used to rigidize the membrane is an aqueous suspension of sub-micron zirconia particles. The combination of mats are submerged in a container of rigidizer, then placed under a vacuum to evacuate the pores. Once pores are relieved of gaseous fillers, the rigidizer infiltrates the pores.

In previous manufacturing, after the infiltration step, the membrane(cloth plus aqueous suspension of sub-micron zirconia particles) was placed on a flat Teflon surface, covered with weighing paper, and constrained from curling by a metal mesh. More recent techniques relied on the wet matrices being placed atop a thin wire bent into a square configuration and attached to a speed controlled rotor; the rotating of the free body should allow a faster more uniformly dry body(matrices) compared to previous techniques.

Once dry, the membrane is analyzed for void fraction and reprocessed if found unacceptable. In the cell, the 65% porous membrane with infiltrated electrolyte prevents cross-over of harmful amounts of hydrogen and allows a low-resistance path for sulfide diffusion and migration. In order to reach such porosity, the method of rigidization must be performed several times, each reducing the porosity by approximately 10%. Every cycle requires drying, placing

mechanical stress on the membrane. The fabricated membrane meeting the 65 % porosity performed adequately in full- cell testing[18].

Thus far improvements in laboratory-densified manufacturing techniques consist of: i) Adding zirconia rigidizer into a knit-zirconia matrix under an extended vacuum (>5 min.). This drastically decreases porosity , reducing the number of steps required to fabricate the membrane. ii) Suspending the mat during drying to increase diffusion since both faces of the mat are exposed, decreasing solvent diffusion distance and iii) vertically rotating the suspended body to uniformly distribute the suspension of zirconia particles throughout the membrane.

Preliminary manufacturing using the rotary dryer failed due to handling problems; Figure 3 reveals an S.E.M. view of membrane cracks connected to these problems. Improvements in the process between steps i and ii are being handled with a more efficient rotor frame, stabilizing the cloth mat prior to the infiltration of the zirconia particles therefore creating a more desirable transition from the vacuum chamber to the rotary drying stage. Processing of membranes with this technique will continue.

Figure 3. S.E.M. View of a Self-Fabricated Zirconia-Cloth Membrane

Dry Pressing

Dry pressing of sub-micron zirconia particles with a percentage of binding material corresponding to a desired porosity has been attempted. Stages in dry pressing include i) the filling of a circular 3 inch diameter carbon steel die with the zirconia particle binder mixture, ii) compacting and shaping of the zirconia binder admixture, and iii) ejection of the pressed disk. Pressing can be accomplished by uni-axial pressing Figure 4a or isostatic pressing Figure 4b. Uni-axial pressing was the technique of choice for initial compression experiments due to ease and availability.

In dry-pressing , pressure produced by moving the die punches compacts the zirconia-binder powder mixture into a cohesive disk with a certain shape and micro-structure according to the extent of applied pressure and binder content. Generally pressures range from 10 - 200 MPa although above 10 MPa rate of densification decreases rapidly; binder content is between 2 and 12 vol% [20]. Dry-pressing of the zirconia-methocel system was accomplished with a pressure of 20 MPa and a binder content of ~ 50 vol%. A high membrane porosity necessitates a higher than normal binder content although inherent problems in binder burnout are inevitable.
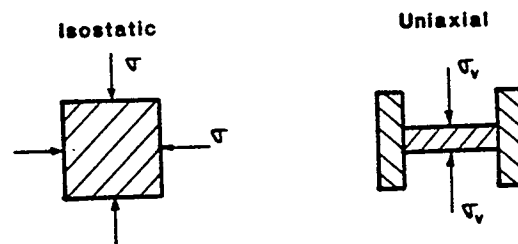

Figure 4. Dry-Pressing with an a) Isostatic Stress Loading and b) Uni-axial Stress Loading

Initial attempts at membrane manufacture by dry-pressing showed promise. Figure 5, an S.E.M. view of the sintered dry-pressed zirconia membrane, reveals an acceptable membrane surface and pore distribution; membrane porosity was ~ 60 % with an average pore size of 1 micron. Work must continue on obtaining a more uniform membrane surface creating parallelism between the membrane and electrode, housing materials as well as alleviating stress fractures during binder burnout and sintering which leads to cracks. Also reduction in membrane thickness must be addressed in order for the dry-pressed membranes to be a viable options for E.M.S. bench-scale experiments; three experiments yielded a membrane of thickness ~ 0.2 cm. Previous membranes utilized successfully in the E.M.S. removal system had a thickness of ~ 0.5 mm.

Figure 5. S.E.M view of a Dry-Pressed Membrane

12

Tape casting

Tape casting is the process of forming a film of controlled thickness under a blade onto a supported substrate. Tape-casting provides a smooth membrane surface as well as a thin (0.01 - 1 mm), flat, uniform, and somewhat compressible membrane [20]. Membranes produced by dry-pressing and extrusion have a less smooth surface below 2 mm in thickness, consist of breakage, non-uniform density, and a non-parallelism between surfaces can be a problem; therefore tape cast membranes if manufactured properly could produce viable membranes for the E.M.S. system, shown in Figure 6.

Tape-casting can be performed continuously or as a batch process. Industrial applications utilize the high volume capacity from continuous casting for multilayer ceramic electronic packaging, multilayer capacitors, piezoelectric devices, thick and thin film insulators, and catalyst supports[20]. Low volume bench-scale requirements (i.e. electrochemical matrices) are ideal for batch production. Examples of batch components used industrially and on our bench-scale membranes are given in Table I and II respectively.
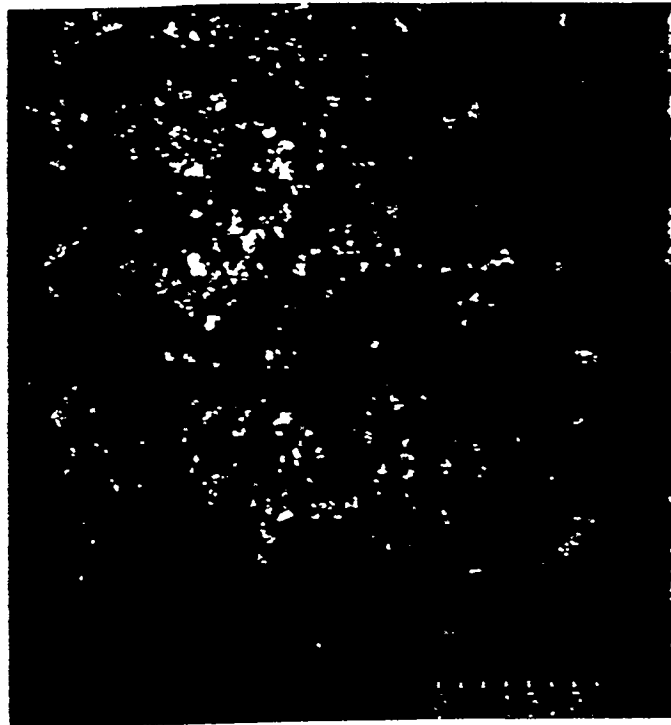

Figure 6. S.E.M. of Tape-Cast Membrane for Bench-scale Experimentation

13

Table I. Examples of Compositions of Tape-Casting Slurries[20] (Industrial)

Component	Alumina Tape	Comp. (vol%)	Titanate tape	Comp. (vol%)
Ceramic powder	Alumina powder*	27	Titanate powder*	28
Liquid system	Trichlorethylene	42	Methylethyl ketone	33
	Ethanol	16	Ethanol	16
Deflocculant dispersant	Menhaden fish oil	1.8	Menhaden fish oil	1.7
Binder	Polyvinyl butyral	4.4	Acrylic	6.7
Plasticizer	Polyethylene glycol	4.8	Polyethylene glycol	6.7
	Octyl phthalate	4.0	Butyl benzyl phthalate	6.7
Surfactant			Cyclohexanone	1.2

* < 5μm, includes sintering aids, grain growth inhibitor

Table II. Example of Composition of Tape-Casting Slurry (Bench-Scale)

Component	Zirconia Tape	Comp. (vol%)
Ceramic powder	Zirconia powder*	16.3
Liquid system	Toluene	47.9
	Denatured Ethyl alcohol	13.2
Deflocculant dispersant	M-111X	4.5
Binder	Vinyl	8.9*
Plasticizer	Unknown	4.6*
Surfactant	Unknown	4.6*

* compositions are a best guess from characteristic values given by metoramic sciences, inc., see Table IV

Borosilicate membranes

Alternate matrix materials also have been investigated including microporous glass membranes with porosities of 0.2 and 0.02 microns, shown in Figure 7 and a thickness of 60 microns exceeding the probable limit of the bench-scale E.M.S. set-up provisions; thus far, these membranes have shown chemical instabilities with the electrolytic melt. Several experiments to

14

illuminate the chemical stability of these membranes in the molten salt electrolytic melt showed a trend of membrane dispersion throughout the melt. Without a stable matrices to entrain the electrolyte, leakage will occur reducing the ionic pathway between electrodes which is detrimental to E.M.S. performance. Future tests with these membranes are not scheduled.
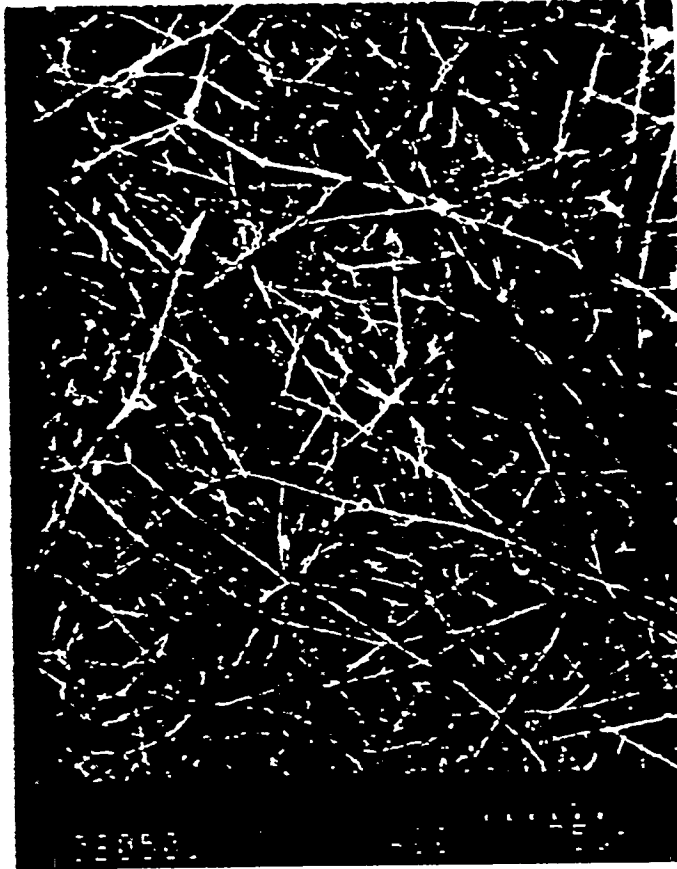

Figure 7. S.E.M. View of a Borosilicate Membrane

Membrane Thickness

Once effective membranes have been developed, other variables such as thickness of the membrane will be investigated in high-flow rate experiments in order to lower the resistance to sulfide migration. The rate of mass transport corresponding to sulfide migration through the membrane is given by:

$$i = \frac{nFD \ (C_c - C_a)}{\delta} \qquad\qquad (3)$$

where n is the charge number, F is Faraday's constant, D is diffusion coefficient, δ is the membrane thickness, and C is the concentration of sulfide species at the cathode and anode. At high process-gas flow rates, mass transfer from the gas is equivalent to the limit of diffusion through the membrane, given by:

$$i_l = \frac{nFD \ C_c}{\delta} \qquad\qquad (4)$$

The limiting current is a measure of the maximum rate at which sulfide can be transported through the membrane, and occurs when $C_a = 0$. Equation (4) reveals that a thinner membrane creates a higher limiting current for the transport of sulfide. This is extremely important at high flow rates to insure diffusion from the bulk process-gas is the only limiting factor.

Optimization of membrane thickness and porosity will be investigated at high flow rates during full-cell testing using a singular laboratory-densified membrane, thickness ~0.38 mm (0.015 in) as well as tape cast and dry-pressed membranes discussed earlier.

Quarterly Summary

Membrane manufacturing coupled with full-cell experimentation was the primary focus this quarter. Zirconia-cloth-stabilization, dry-pressing, and tape-casting manufacturing methods were used. Table III gives an outline of membrane materials as well as other components for each experiment.

Three full-cell experiments (runs 20 - 22) served a two-fold purpose: 1) testing the electrochemical membrane separators ability to concentrate CO_2; and 2) testing modifications of the experimental apparatus.

Table III. Experimental Components

Run	Temp. ^oC	Cathode	Anode	Membrane	Housings	Electrolyte
20	650	Ni	NiO	Tape-cast (ZrO_2)	MACOR	$(Li_{0.62}K_{0.38})_2CO_3$
21	650	Ni	Ni	Dry-pressed (ZrO_2)	MACOR	$(Li_{0.62}K_{0.38})_2CO_3$
22	650	Ni	Ni	Pre-fabricated (ZrO_2)	Stainless steel (316)	$(Li_{0.62}K_{0.38})_2CO_3$

Run #20

A ZrO_2 tape-cast membrane was used for the first time in the E.M.S. system. The slurry consisted of 10 grams ZrO_2 powder (d_p ~ 0.2 μm) mixed with 7.5 grams of a binder-solvent system (B-73305, characteristics of which are given in Table IV), coupled with 0.1 grams of surfactant/dispersant (M-1114). Mixture of the ceramic, binder-solvent system is based on the desired membrane characteristics; optimal porosity is in the 50 to 70% range with pore diameters of 0.1 microns.

Table IV. Characteristics of the Metoramic Science Binder-Solvent System B-73305

Resin Type	Vinyl
Typical Composition (wt%)	61.3 Toluene
	15.3 Denatured ethyl alcohol
	23.4 Other additives: polymer, surfactants, plasticizers, adhesion, and porosity modifiers
Typical Properties	Binder solids 22.3 wt%
	Binder Viscosity 550 cps
	Binder Specific Gravity 0.88
	Binder Solids Specific Gravity 1.0
	Wt per Gallon 7.33 lbs. (3.33 kg)
Appearance	Clear to slightly hazy-yellow solution

The ceramic loading into the binder-solvent system necessary for obtaining a ceramic matrices of 50% porosity is calculated as follows:

$$\text{Grams of B73305} = \left(\frac{\text{grams of ZrO}_2}{\text{density of ZrO}_2 \left(\frac{\text{grams}}{\text{cm}^3} \right)} \right) \times \left(\frac{\text{density of binder solids} \left(\frac{\text{grams}}{\text{cm}^3} \right)}{\text{wt\% binder solids} \left(\frac{\text{grams of binder solids}}{\text{grams total}} \right)} \right) \quad (5)$$

A membrane of 50% porosity was successfully manufactured in a batch-wise process.

The 3 grams of electrolyte needed to saturate the ceramic membrane was pressed uni-axially into a 7.6 cm diameter disk at 5 MPa prior to cell assembly.

Porous cathode and anode Ni electrodes were obtained from MemTec and Energy Research Corporation.. Both electrodes were oxidized and lithiated at 600 C. S.E.M. analysis of both materials is shown in Figure 8 and 9. A cobalt cathode produced for run #20 cracked during installation; however Figure 10 shows that the morphology of the electrode material was suitable for full-cell experimentation when compared to the substituted ERC Ni electrode, Figure 9. Since Ni was used to replace Co as a cathode material H_2S levels over 50 ppmv could not be applied to the cell due to the phase transition previously evidenced from solid-conductive Ni to the molten-conductive $Ni_{3+x}S_2$.

Figure 8. S.E.M. View of a MemTec Ni Electrode (Pre-lithiated and Oxidized to NiO)
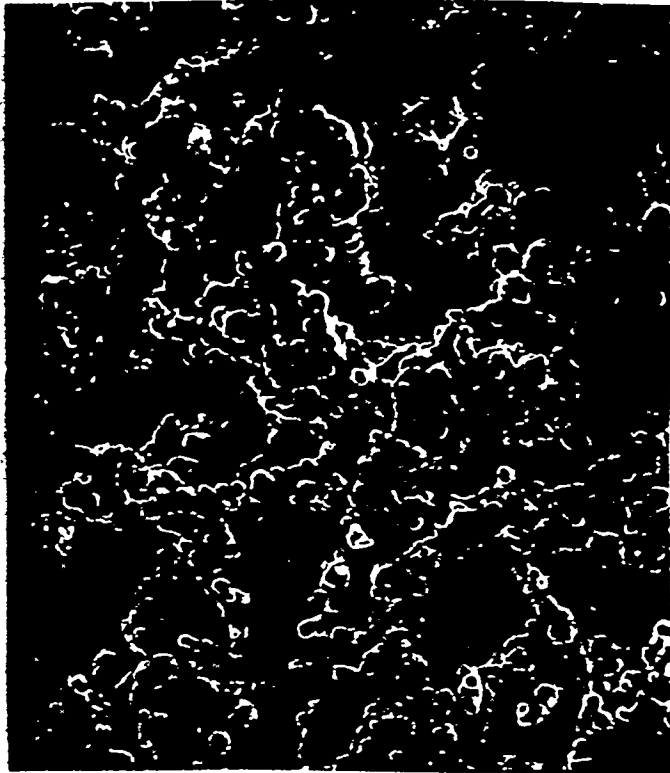
Figure 9. S.E.M. View of an E.R.C. Ni Electrode

Figure 10. S.E.M. View of Laboratory Fabricated Cobalt Electrode

Upon full-cell start-up the initial temperature was set at 400 C. Binder-burnout was evidenced by smoke and organics in the exhaust. Cathode and anode gas flow rates were 218 cc/min N_2 and 60 cc/min N_2 respectively. Binder volatiles were still apparent after holding the temperature at ~ 470 C (just below the electrolytic melting point of 490 C) for 12 hours. A temperature increase to 590 C resulted in electrolytic melting coupled with total process-gas seal development (i.e. volumetric flow in = volumetric flow out). Cathodic flow was adjusted to 243 cc/min; 108 cc/min was comprised of fuel gas (18% CO_2, 45% CO, and 37% H_2) and the remaining 136 cc/min of N_2. The anodic inlet gas consisted of 75 cc/min N_2.

Evaluation of theoretical CO_2 removal from the process-gas (cathode-gas) with applied current was the first test conducted on the Electrochemical Membrane Separator (E.M.S.) full-cell run; percentage of CO_2 removal compared to the theoretical value determines system permanence. Application of 200 mA to the cell caused process-gas CO_2 levels to decrease by 85% of the theoretical value. 100% of the theoretical value is necessary before H_2S application. Internal resistance was ~ 6Ω; an acceptable value is 1Ω.

Several factors lead to the demise of run #20: i) Binder burnout continued throughout experimentation and eventually caused clogging of the anode outlet tube; ii) Gas cross-over was apparent due to membrane damage; and iii) Faulty current collectors created consistent instabilities in CO_2 removal. Attempts were made to unclog the anode tube by plunging with an acetone saturated cotton swab; however these efforts failed due to continually escaping volatiles from the system. Shut-down eventually occurred after 50 hours of operation due to electrical connection failure; a deficiency of electrolyte or current collector breakage caused the problem.

Post-mortem analysis revealed the platinum current collector on the cathode side was broken severing electrical contact. Gas cross-over occurred via cracks in the membrane due to the concave design in the anode electrode well.

Although H_2S removal was not attempted with this experiment the cell apparatus proved acceptable for future full-cell experimentation.

Run #21

A dry-pressed membrane was incorporated into the E.M.S system for the first time. 14.13 grams of ZrO_2 powder ($d_p \sim 0.2$ μm) was mixed with 4.13 grams of methocel in a ball-mill then pressed into a disk 7.6 cm diameter at 5 MPa. The ZrO_2-methocel disk was placed atop a 15.3 cm diameter ceramic disk then covered by a square ceramic piece 5.1 cm squared. Temperature cycling for binder burnout consisted of the following:

1) Ramp up to 650 C at a rate of 1 C/min -> dwell for 2 hours

2) ramp up to 1200 C at a rate of 1 C/min -> dwell for 1 hour

3) ramp down to 25 C at a rate of 1 C/min

Additional binder-burnout occurred with the membrane placed atop a refractory brick and heated to 500 C. After manufacture, membrane characteristics consisted of a 2.3 mm thickness (~ 0.5 mm is desirable), 650 mm diameter, and a porosity of ~ 68% (porosities of ~ 65% have shown the best results to date). 12 grams of electrolyte pressed into a disk 3 inches in diameter was utilized for cell construction. Ni, used for both cathode and anode, was obtained from Energy Research Corporation (ERC), Figure 9.

Problems associated with the experimental apparatus caused shut down to occur before data was acquired. The oven temperature dropped well below the electrolytic melting point twice creating more stress than the membrane could withstand due to incompatible thermal expansion coefficients. Shut-down occurred after ~ 27 hours of operation.

Post-mortem analysis revealed a major crack in the membrane. Both electrodes were flooded with electrolyte.

Run #22

The ZrO_2 membrane used was manufactured by Zircar with a porosity of 67%, thickness of 0.5 mm, pore diameter of 0.1 microns, and an area 5.1 cm squared. 3.5 grams of electrolyte corresponded to membrane void volume saturation. ERC supplied the Ni anode and cathode materials which were doped with lithium ions to improve electrode conductivity.

Once cell components were in place the housings were bound together to insure stability upon cell installation into the oven. Process gas seals were apparent prior to the electrolyte melting temperature (470 C) due to 1400 grams placed atop the cell. Once the cell reached a temperature of 600 C anode inlet flow equated to outlet flow (~47 cc/min N_2) while the process inlet flow of 93 cc/min N_2 and 57 cc/min fuel gas (18% CO_2, 45 % CO, and 37% H_2) did not match the outlet flow of 93 cc/min indicating external gas loses. No bulk gas flow through the membrane was evident.

50 mA applied to the cell resulted in 0% CO_2 removal with an internal resistance across the membrane of 3Ω and a potential of 0.8 V. To decrease internal resistance, 3 grams of electrolyte were added. The potential at zero current was 0.340 V (cathode to anode). Upon application of 100 mA, approximately 40% of the CO_2 theoretically predicted was removed from the cathode side and 35% of the predicted CO_2 evolution occurred on the anode side. This same trend of removal and evolution continued throughout the run as well as a continual increase in polarization (~2 mV/sec). Further addition of electrolyte eventually resulted in 100% CO_2 removal at the cathode with an IR of 1Ω; however, anode CO_2 evolution remained unchanged.

Once again the experimental apparatus created problems leading to shut-down of the system prior to H_2S addition. Failure of the heating elements inside the oven caused internal oven temperature to drop to ~200 C, well below the eutectic melting point of 490 C. Attempts were made to reheat the system with minor success. All seals remained intact throughout thermal cycling. Erratic potentials upon application of current continued, possibly due to mass transfer effects associated with either electrode pore flooding or a deficiency in electrolyte. Post mortem analysis revealed the prior to be the case. Further experiments must investigate the relationship of membrane and electrode pores for proper electrolytic distribution in the E.M.S. system. Shut-down occurred after 168 hours.

Conclusion

The Fossil Energy Advanced Research Program requires high temperature separations to remove environmental contaminants from post-combustion flue gases as well as pre-combustion process gases. This project is aimed at the latter: the removal of hydrogen sulfide from coal gas at gasifier temperatures. This development would enable a simplification of the entire gasification scheme by permitting a one-step removal of hydrogen sulfide and production of elemental sulfur. Energy savings accrue due to the high temperature processing.

The DOE programs relating to gasification for power production have as their goal the more efficient, clean paths toward affordable energy from coal. Gas clean-up accounts for nearly one-third of the cost of this conversion. Simplification and economization will benefit the entire effort.

Project Output

Current experiments are based on improving selective removal from low initial H_2S concentrations (100 ppm and 20 ppm H_2S). High flow rate effects, membrane stability and selectivity, and electrode morphology characterizes present studies, with recent results showing over 90% H_2S removal with applied current.

Experimental results presented are based on two experiments with initial H_2S concentrations of 100 ppm and 20 ppm. To represent probable industrial conditions, variables such as flow rates, selectivity of the membranes, and process-gas seals, were of primary concern in these experiments. Maximum removals of H_2S are reported on a zero current basis, thus compensating for any chemical scrubbing effects of the non-equilibrium electrolyte species in the membrane. Percent H_2S removal with applied current exceeded 80% and in some cases reached 90%, given by:

$$\%H_2S \text{ Removal} = \frac{\left(\text{Outlet } H_2S_{zero\ current} - \text{Outlet } H_2S_{applied}\right)}{\left(\text{Outlet } H_2S_{zero\ current}\right)} \times 100 \qquad (6)$$

Cell housing materials used for both experiments were a machineable ceramic (MACOR). Cathode and anode electrodes consisted of Ni, oxidized in situ to form NiO. Process-gas seals developed, in-situ, by placing aluminum foil gaskets on both sides of the electrolyte filled membrane. Al oxidation initially forms Al_2O_3 which on reaction with Li, contained in the electrolyte, forms $LiAlO_2$.

The membrane for the 100 ppm experiment, used two tapes of MgO and one mat of zirconia cloth. Acrylic binders used in the MgO tapes (Metoramics K565-4 binder system) were burned out under an O_2 atmosphere at 350°C and the $(Li_{0.62}K_{0.38})_2CO_3$ eutectic-composition electrolyte was added with the cell at run temperature. Inlet gases were passed through a stainless steel shift reactor, allowing them to equilibrate before passing through the cell. Gas compositions at 973K after the shift reactor were 14.3% CO_2, 50.8% CO, 4.8% H_2O, 30.1% H_2, and 100 ppm H_2S.

H_2S removal vs. applied current, with a cathodic flow rate of 88 cc/min., is presented in Figure 11. H_2S removals of 90% were achieved with H_2S current efficiencies of 5%.

The membrane for 20 ppm experiments was purchased from Zircar Corporation, consisting of yttria-stabilized zirconia in a rigid form at 66% porosity. The advantages of these membranes are consistently uniform porosities and no warping. A cold pressed disk of the Li/K eutectic carbonate electrolyte, placed between the cathode housing and the Zircar membrane, provided a stable start-up configuration. Inlet gases equilibrated to 5.8% CO_2, 25.6% CO, 6.7% H_2O, and 65.3% H_2, after the water-gas shift reactor. The electrolyte sulfide concentration equilibrated in-situ to 0.11 mole%.

Temperature remained constant (650°C) while flow rates varied from 170 cc/min. to 814 cc/min. H_2S removal at all flow rates exceeded 80% with applied current as shown in Figure 12; Current efficiencies were ~ 35%.
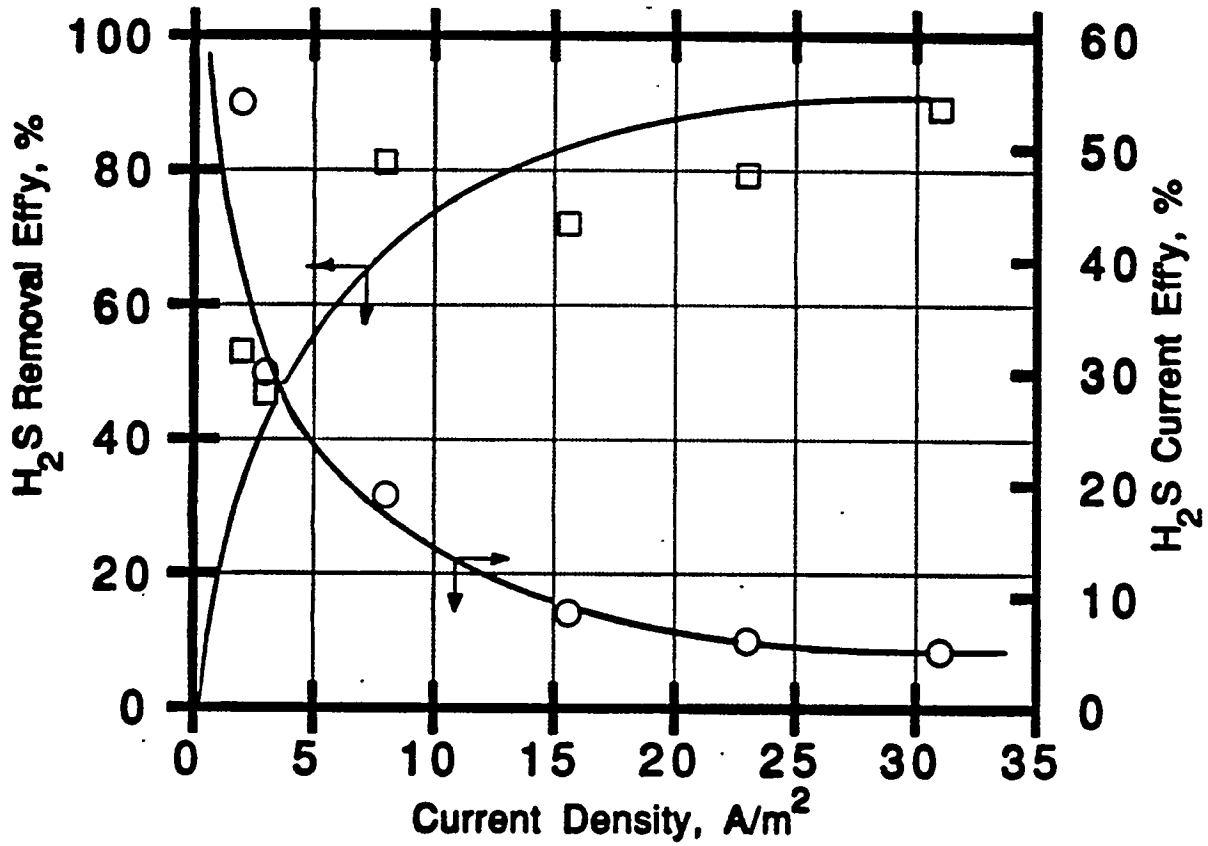
Figure 11. H$_2$S Current and Removal Efficiency vs. Current Density; 100 ppm inlet H$_2$S
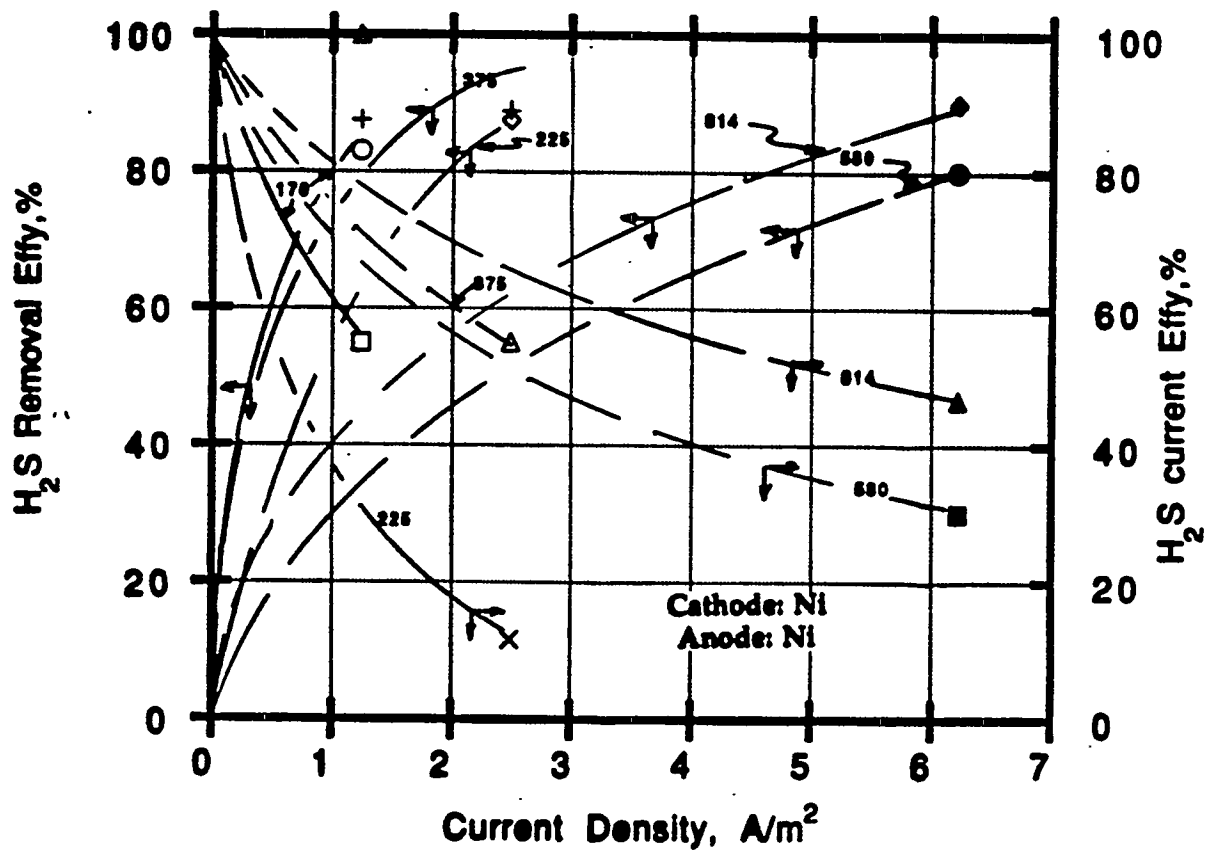
Cathodic Flow Rate = 88 cc/min

Figure 12. H2S Current and Removal Efficiency vs. Current Density; 20 ppm inlet H2S

Parametric values are in cc/min

References

1.   U.S. Dept of Energy, DOE/METC 87/0255, DE87006493, Oct., 1987.

2.   Skerret, P.J., "Fuel Cell Update", *Popular Science*, 89-91, 120-1, June, 1993.

3.   Lim, H.S. and Winnick, J., *J. Electrochem. Soc.*, **131, 562-8** (1984).

4.   Alexander, S., and Winnick, J., *1990 AIcHE Annual Meeting*, Chicago, IL., 1990.

5.   Alexander, S., and Winnick, J., *Sep'n Sci. and Tech.*, **25**, 2057-72 (1990).

6.   Weaver, D., and Winnick, J., *J. Electrochem. Soc.*, **134**, 2451-58 (1987).

7.   Weaver, D., and Winnick, J., *J. Electrochem. Soc.*, **138**, 1626-37 (1991).

8.   Banks, E., and Winnick, J., *J. Appl. Electrochem.*, **16**, 583-90 (1986).

9.   White, K.A., and Winnick, J., *Electrochim. Acta*, **30**, 511-516 (1985).

10. EPRIEM-1333, *Assessment of Sulfur Removal Processes for Advanced Fuel Cell Systems, Final Report,* C.F. Braun and Co., Alhambra, CA, Jan., 1980.

11. Vidt, E.J., DOE/METC DE-AC-21-81MC16220, DE82013942, Westinghouse, Dec., 1981.

12. Focht, G.D. et. al., DOE/MC/121166-2163, DE86016041, July, 1986.

13. Lyke, S.E., DOE/MC/19077-1803, DE8500961, Battelle Pacific Northwestern Laboratories, Jan. 1985.

14. Winnick, J., Quarterly Progress Report #13, DOE grant DE-FG-91PC91288.

15. Winnick, J., Quarterly Progress Report #11, DOE grant DE-FG-91PC91288.

16. Weaver, D., and Winnick, J., *J. Electrochem. Soc.*, **139**, 492-498 (1992).

17. Alexander, S., *Ph.D. Thesis*, Georgia Institute of Technology, Atlanta, GA, 1992.

18. Winnick, J., Quarterly Progress Report #6, DOE grant DE-FG-91PC91288.

19. Winnick, J., Quarterly Progress Report #8, DOE grant DE-FG-91PC91288.

20. Reed, James S., Introduction to the Principles of Ceramic Processing, John Wiley & Sons, New York, 1988.